Specific expression and function of inositol 1,4,5-trisphosphate 3-kinase C (ITPKC) in wild type and knock-out mice

Ariane Scoumanne [a,1], Patricia Molina-Ortiz [a], Daniel Monteyne [b], David Perez-Morga [b,c], Christophe Erneux [d], Stéphane Schurmans [a,*]

[a] Laboratoire de Génétique Fonctionnelle, GIGA-B34, Université de Liège, avenue de l'Hôpital 11, 4000 Liège, Belgium
[b] Laboratoire de Parasitologie Moléculaire, Institut de Biologie et de Médecine Moléculaires (IBMM), Université Libre de Bruxelles, rue des Professeurs Jeener et Brachet 12, 6041 Gosselies, Belgium
[c] Center for Microscopy and Molecular Imaging (CMMI), Université Libre de Bruxelles (ULB), 8 rue Adrienne Bolland, B-6041 Gosselies, Belgium
[d] Institut de Recherches Interdisciplinaires en Biologie Humaine et Moléculaire (IRIBHM), Campus Erasme, Université Libre de Bruxelles, route de Lennik, 808, 1070 Bruxelles, Belgium

ARTICLE INFO

ABSTRACT

Inositol 1,4,5-trisphosphate 3-kinase C (ITPKC) is the last identified member of the inositol 1,4,5-trisphosphate 3-kinases family which phosphorylates inositol 1,4,5-trisphosphate into inositol 1,3,4,5-tetrakisphosphate. Although expression and function of the two other family members ITPKA and ITPKB are rather well characterized, similar information is lacking for ITPKC. Here, we first defined the expression of *Itpkc* mRNA and protein in mouse tissues and cells using *in situ* hybridization and new antibodies. Surprisingly, we found that cells positive for ITPKC in the studied tissues express either a multicilium (tracheal and bronchial epithelia, brain ependymal cells), microvilli forming a brush border (small and large intestine, and kidney proximal tubule cells) or a flagellum (spermatozoa), suggesting a role for ITPKC either in the development or the function of these specialized cellular structures. Given this surprising expression, we then analyzed ITPKC function in multiciliated tracheal epithelial cells and sperm cells using our *Itpkc* knock-out mouse model. Unfortunately, no significant difference was observed between control and mutant mice for any of the parameters tested, leaving the exact *in vivo* function of this third Ins(1,4,5)P3 3-kinase still open.

© 2016 Elsevier Ltd. All rights reserved.

---

1. Introduction

Inositol 1,4,5-trisphosphate (Ins(1,4,5)P3), the well-known calcium mobilization messenger, can be phosphorylated into inositol 1,3,4,5-tetrakisphosphate (Ins(1,3,4,5)P4) by Ins(1,4,5)P3 3-kinases (Itpk) isoforms a, b and c, or by Ipk2/Ipmk, the inositol phosphate multikinase (Choi et al., 1990; Takazawa et al., 1990, 1991; Dewaste et al., 2000; Saiardi et al., 2000; reviewed by York, 2006). The a, b and c isoforms of Ins(1,4,5)P3 3-kinases (or ITPKA, ITPKB and ITPKC) share a well conserved carboxy-terminal catalytic domain, an ATP binding motif, an inositol binding motif, and a calmodulin binding domain (reviewed by Erneux et al., 2016). All three Ins(1,4,5)P3 3-kinase isoforms have been shown to be sensitive to Ca^{2+} to various degress; their activity is also regulated by direct protein phosphorylation (Communi et al., 1997). Tissue expression of these 3 isoforms has been previously reported: using Northern blotting and RT-PCR, *Itpkc* mRNA has been shown to be rather ubiquitously expressed in human and mouse tissues, as *Itpkb* (Vanweyenberg et al., 1995; Dewaste et al., 2000). However, the precise cellular localization of endogenous ITPKC in these tissues has never been reported in the literature, as no specific antibody has been reported to detect the endogenous protein. Production and analysis of mice genetically-deficient for *Itpka* and *Itpkb* have strongly helped to characterize the *in vivo* functions of these enzymes and the corresponding mechanisms of Ins(1,3,4,5)P4 action (Pouillon et al., 2013; Schurmans et al., 2011, 2015). By contrast, the physiological function of ITPKC is poorly characterized *in vivo*: *Itpkc*-deficient mice have been generated in our laboratory, but these mice appear healthy with a normal lifespan and growth (Pouillon et al., 2003). No gross morphological alterations have been detected in organs isolated from these mice. T cell development and calcium response following stimulation were found to be normal in these knock-out mice. Furthermore, inactivation of *Itpkc* on an *Itpkb*$^{-/-}$ genetic background did not demonstrate additional T cell alterations beyond those of *Itpkb*$^{-/-}$ mice, excluding a potential compensatory mechanism by the b isoform to explain the absence of obvious phenotype in *Itpkc*$^{-/-}$ mice (Pouillon et al., 2003). Interestingly, an *ITPKC* functional genetic polymorphism was discovered to be associated with Kawasaki disease susceptibility (Onouchi et al., 2008). Kawasaki disease (KD) is a severe and acute pediatric systemic vasculitis of unknown etiology. KD may lead to formation of coronary artery aneurysms and to ischemic heart disease, myocardial infarction and sudden death (Hata and Onouchi, 2009). The link between this *ITPKC* polymorphism and KD (or resistance to KD treatment) was confirmed in other studies, but others failed to reproduce these results and no association of the *ITPKC* locus with KD was detected (Burgner et al., 2009; Khor et al., 2011; Kuo et al., 2011; Lin et al., 2011; Onouchi et al., 2013; Peng et al., 2012).

In order to better characterize the C isoform of the Ins(1,4,5)P3 3-kinases family, we defined the expression of *Itpkc* mRNA and protein in mouse tissues and cells using *in situ* hybridization and new antibodies. Then, based on these expression studies, we analyzed Itpkc function in specific cells using our *Itpkc* knock-out mouse model.

2. Materials and methods

2.1. Mice

Itpkc$^{-/-}$ mice were generated in our laboratory (Pouillon et al., 2003). Mice were maintained in a specific pathogen free facility at the GIGA-research Center. *Itpkc*$^{-/-}$ and wild-type mice between 6 and 12 weeks of age were used in this study. All procedures involving mice were approved by the Animal Care and Use Review Committee of the Université de Liège.

2.2. Antibodies

Affinity purified anti-mouse ITPKC polyclonal antibodies named GS2 and GS4 were made by immunizing rabbits with peptide LPERDNKPRVDNLRC and QPGSDGFSS KDTESC, respectively (GenScript). Affinity purified anti-mouse ITPKC antibody named Ald was produced by immunizing rabbits with three peptides: RGGRRRQPGLQRPGPGAG, KPRQNKELDGSNLQTHPRRN-C and SQTDDSLKGPSTQTAC (Aldevron). Those peptides were chosen in the sequence of mouse ITPKC (Pouillon et al., 2003). Specificity of detection was confirmed by Western blot and immunofluorescence analysis using anti-ITPKC antibodies pre-incubated or not with their corresponding immunizing peptides.

Anti-ezrin antibody was obtained from ThermoFisher Scientific. Anti-centrin was purchased from Millipore. Anti-acetylated tubulin, phalloidin-TRICT and anti-gamma tubulin were obtained from Sigma−Aldrich. Rabbit IgGs and mouse IgGs were from Santa Cruz Biotechnologies. Anti-rabbit IgGs Atto 488 and Atto 594-conjugated secondary antibodies were obtained from Sigma−Aldrich. Horse-radish peroxidase (HRP)-conjugated secondary antibodies were obtained from Santa Cruz Biotechnologies.

2.3. Immunodetection by Western blotting

To prepare mouse tissue lysates, fresh tissues were snap-frozen in liquid nitrogen, suspended in protein lysis buffer with Protease Inhibitors Cocktail (PIC) tablets (Roche) using an homogenizer (VDI 12, VWR) or a pestle and incubated at 95 °C for 5 min. After centrifugation at 10,000 × g for 5 min, protein of tissue lysates were quantified and 60 μg of lysates were used for Western blot analysis. To prepare MTEC lysates, MTEC cultured on Transwell inserts were washed with PBS, suspended in lysis buffer with PIC and incubated at 95 °C for 5 min. After quantification, 60 μg of cell lysates were used for Western blot analysis. Briefly, SDS-PAGE was performed and transferred to nitrocellulose membrane using the Trans-blot Turbo transfer system

(BioRad). Membranes were blocked with PBS containing 5% non-fat milk and 0.1% Tween-20 for 1 h and incubated with primary antibodies in PBS containing 2% non-fat milk and 0.1% Tween-20 at 4 °C overnight. After 3 washes, the membranes were incubated with HRP-conjugated secondary antibodies for 1 h, washed and revealed with enhanced chemiluminescence (ECL) onto Hyperfilm (Amersham). Images were quantitated with Image J software (National Institutes of Health).

2.4. HEK cell culture and transfection

HEK cells were cultured in DMEM medium supplemented with 10% FBS, 2% Penicillin-Streptomycin, 0.1 mM MEM-Non Essential Amino-Acids and 2 mM L-glutamine (Gibco) in an incubator with 5% CO_2 at 37 °C. For transient transfection, cells were seeded at 10^6 cells per well in a 6-well plate and transfected with FuGENE 6 transfection reagent (Promega), using 1 μg pCMV6-m*Itpkc* cDNA vector (OriGene BC053450) in 40 μl serum-free Opti-MEM (ThermoFisher Scientific) combined with 6 μl FuGENE 6. After 24 h, transfected cells were washed with PBS and harvested in 50 μl lysis buffer with PIC for Western blot or immunofluorescence analysis.

2.5. RTqPCR on mouse tissues

Mouse tissues were collected and snap-frozen in liquid nitrogen. Total RNA was extracted using RNeasy Mini Kit (Qiagen) and cDNA was synthesized using iScript (BioRad). To determine *Itpkc* mRNA levels, qPCR was performed on an iQ5 real-time PCR detection system (BioRad) in a total volume of 20 μl containing 50 nM primers and $1\times$ iQ SYBR Green Supermix (BioRad). For *Itpkc* amplification, primers m*Itpkc*-F (5′-CTG AAG TAC TCG CCC TTC GT-3′) and m*Itpkc*-R (5′- TGC TCA CAC TGA CAG AAA CG-3′) were used. For 18S amplification, primers 18S-F (5′- GCA ATT ATT CCC CAT GAA CG-3′) and primers 18S-R (5′-AGG GCC TCA CTA AAC CAT CC-3′) were used.

2.6. Isolation and culture of mouse tracheal epithelial cells (MTEC)

MTEC culture was based on the report of You et al. (2002). Briefly, mice were killed and tracheas were excised and trimmed of excess tissues. Tracheas were opened longitudinally to expose the lumen and incubated in DMEM/F12 medium (ThermoFisher Scientific) containing 1.5 mg/ml pronase (Roche) at 4 °C for 18 h. Tracheal epithelial cells were dislodged by gentle agitation and collected in DMEM/F12 medium. The cells were treated with 0.5 mg/ml DNAse I (Sigma−Aldrich) on ice for 5 min and centrifuged at $400 \times$ g at 4 °C for 5 min. The cell pellet was suspended in DMEM/F12 medium containing 10% FBS, plated in a T75 flask and placed in an incubator at 37 °C and 5% CO_2 for 2 h to allow adherence of contaminating fibroblasts. Non-adherent cells were centrifuged, suspended in DMEM/F12 medium supplemented with 10 μg/ml insulin, 5 μg/ml transferrin, 25 ng/ml EGF, 30 μg/ml bovine pituitary extract, 5% FBS and freshly added 0.01 μM retinoic acid. The cells were seeded at 7.5×10^4 cells per cm^2 onto collagen-coated Transwell inserts (Corning) and maintained in an incubator at 37 °C and 5% CO_2. Medium was changed every other day. Once reaching confluence (after ~ 10 days), the culture of undifferentiated epithelial cells was changed to an air-liquid interface culture by adding DMEM/F12 medium containing 2% NuSerum (Corning) to the bottom compartment only (You et al., 2002). MTEC were maintained in an incubator at 37 °C and 5% CO_2 and medium was changed every other day until reaching full differentiation (after ~ 15 days). MTEC were used at air-liquid interface day 15−19 in this study. All media were supplemented with 100 U/ml penicillin, 100 mg/ml streptomycin, 15 mM Hepes and 0.25 μg/ml Fungizone.

2.7. Evaluation of ciliary beat frequency of MTEC

MTEC cultures at air-liquid interface day 17−19 were placed in a 37 °C chamber onto the stage of a Nikon A1R confocal microscope. Time-lapse images were captured at a $40\times$ magnification objective and a frame-rate of 30 frames per sec, for 3 s. The ImageJ software was used to calculate the ciliary beat frequency (CBF): CBF (Hz) = number of cyclical changes in pixel intensity in X frames * (frame-rate/X). Average ± S.D. was calculated from three counting.

2.8. Immunofluorescence and confocal microscopy

For MTEC, cells grown on Transwell inserts were rinsed with PBS, fixed in 10% formalin for 10 min and washed with PBS. Transwell filters were excised from their plastic supports and placed cell-side up on a slide. Filters were blocked in PBS containing 5% goat serum, 3% BSA, 0.1% Triton X-100 and 1/100 dilution of unconjugated anti-mouse IgG antibody (Jackson ImmunoResearch Laboratories) for 1 h. Filters were incubated with primary antibodies diluted in PBS containing 2% goat serum, 1% BSA, 0.1% Triton X-100 for 1 h or overnight at 4 °C. The filters were washed 3 times for 10 min and incubated with fluorochrome-labeled secondary antibodies (Sigma−Aldrich) for 1 h. After 3 washes, the filters were incubated with 300 nM DAPI in PBS (ThermoFisher Scientific) for 5 min. After 3 washes, the filters were mounted using Prolong (ThermoFisher Scientific). Images were acquired using the NIS 4.20.00 software on a Nikon A1R confocal microscope. Image stacks were collected with a z-section of 0.2 μm and were processed using ImageJ (National Institutes of Health).

For mouse tissues, 5 μm cryosections were prepared and mounted on Superfrost Ultra Plus slide. The sections were fixed with acetone for 10 min and blocked in PBS containing 5% goat serum, 0.1% Triton X-100 and 1/100 dilution of unconjugated

anti-mouse IgG antibody (Jackson ImmunoResearch Laboratories) for 1 h or overnight at 4 °C. The sections were incubated with primary antibodies diluted in PBS containing 2% goat serum for 1 h, then washed 3 times for 5 min. The sections were incubated with fluorochrome-conjugated secondary antibodies (Sigma—Aldrich) for 1 h, washed and incubated with DAPI for 5 min. After 3 washes, the slides were mounted in Prolong and images were acquired as described for MTEC.

2.9. In situ hybridization on mouse tissue sections

A mouse *Itpkc* oligo RNAscope probe was designed and provided by Advanced Cell Diagnostic. *In situ* hybridization was performed using the RNAscope Multiplex Fluorescent Assay (ACD). Briefly, fresh tissues were quickly frozen in liquid nitrogen and embedded in OCT medium. Cryosections of 14 μm were prepared and mounted on SuperFrost Plus slides. Sections were fixed and pre-treated according to the RNAscope guide for Fresh frozen Tissue (ACD). Following pre-treatment, the sections were hybridized with the *Itpkc* oligo probe using the HybEZ Hybridization System (ACD). After several amplification sets, the sections were counterstained with DAPI and mounted using Prolong. A Polar2A probe and a bacterial dapB probe were used as positive and negative controls, respectively. Images were acquired using Nikon A1R confocal microscope and image stacks were processed using ImageJ.

2.10. Epididymal spermatozoa isolation and morphology

The epididymis was collected in TYH buffer containing 120 mM NaCl, 5 mM KCl, 1.2 mM $MgSO_4$, 1.7 mM $CaCl_2$, 1.2 mM K_2PO_4, 25 mM $NaHCO_3$, 1 mM sodium pyruvate, 5.6 mM glucose and 20 mM Hepes, pH 7.4 (Burnett et al., 2011). The epididymis was cut and incubated for 15 min at 37 °C to allow the sperm to get out. For capacitation, an equal volume of TYH buffer containing 5% BSA was added and the sperm suspension was incubated at 37 °C for 1 h. For sperm flagellar analysis, the sperm suspension was mixed with equal volume of 2× stimulant solution (0—50 mM Lyral, Sigma—Aldrich) (Fukuda et al., 2004). An aliquot of stimulated sperm suspension was mounted on slide and coverslip. Phase-contrast images were taken using a Nikon Eclipse 90i microscope.

2.11. Scanning electron microscopy (SEM) on mouse trachea

Samples were washed with PBS, fixed overnight at 4 °C in glutaraldehyde 2.5%, 0.1M cacodylate buffer (pH 7.2) and post-fixed in OsO4 (2%) in the same buffer. After serial dehydration, samples were dried at critical point and coated with platinum by standard procedures. Observations were made in a Tecnai FEG ESEM QUANTA 200 (FEI) at 30 kV and images processed by SIS iTEM (Olympus) software.

2.12. Statistical analysis

All values are expressed as means ± standard error of the mean (SEM). Significance of differences between two means was calculated using the GraphPad InStat software (GraphPad Software, San Diego, USA). Significance level of the differences of the means (p-value) is presented.

3. Results and discussion

3.1. Analysis of mouse Itpkc antibodies in HEK cells

Three antibodies, GS2, GS4 and Ald, were obtained after rabbit immunization with different peptides localized in the N-terminal region of the mouse ITPKC protein which is encoded by the first coding exon of the *Itpkc* gene (see Supplementary Material). These antibodies were first tested by immunodetection on protein extracts isolated from HEK cells transfected or not with an expression plasmid for the mouse *Itpkc* cDNA. Using all three antibodies, a strong signal was observed at ~90 kDa in the mouse *Itpkc* cDNA-transfected HEK cell extract; no signal was detected in the non-transfected HEK cell extract (Fig. 1a and Supplementary Fig. 1). This signal was absent or markedly decreased when antibodies were incubated with the corresponding immunizing peptide(s) before addition onto the membrane (Fig. 1a and Supplementary Fig. 1). Second, GS2, GS4 and Ald antibodies were tested for their capacity to detect the mouse ITPKC protein by immunofluorescence on coverslips in mouse *Itpkc* cDNA-transfected HEK cells (Fig. 1b). Only the GS2 antibody detected a homogeneous cytoplasmic staining in ~30% of transfected HEK cells; the staining markedly decreased when the GS2 antibody was incubated with the corresponding immunizing peptide before addition on transfected HEK cells. No staining was detected with the GS2 antibody in non-transfected HEK cells, and no staining was observed in mouse *Itpkc* cDNA-transfected HEK cells using GS4 and Ald antibodies (data not shown).

3.2. Analysis of Itpkc mRNA and protein expression in normal mouse tissues and cells

Fourteen tissues were isolated from a normal adult male mouse; mRNA was extracted from each tissue and reverse-transcribed. cDNAs were then processed for qPCR in order to analyze *Itpkc* mRNA expression (Fig. 1c). Mouse *Itpkc* mRNA
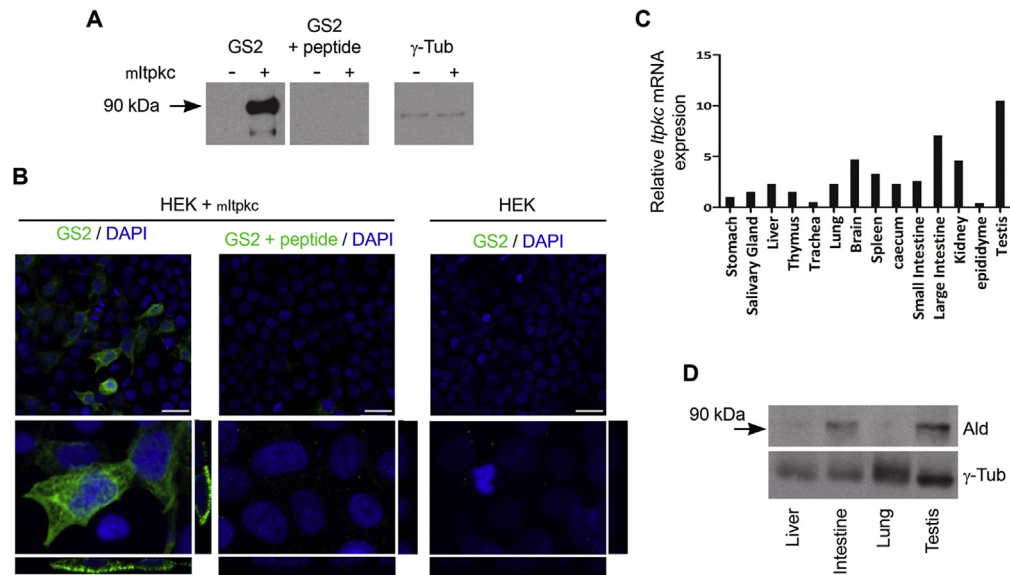
Fig. 1. Analysis of mouse Itpkc mRNA and protein expression in transfected HEK cells and mouse tissues: (A) Immunodetection on protein extracts isolated from HEK cells transfected (+) or not (−) with a mouse *Itpkc* (mItpkc) cDNA expression plasmid. GS2, GS2 preincubated with the immunizing peptide and gamma Tubulin antibodies were added to the membrane. (B) IF studies with GS2 (green) and GS2 preincubated with the immunizing peptide on HEK cells transfected (HEK + mouse Itpkc) or not (HEK) with a mouse Itpkc cDNA expression plasmid. Cells were counterstained with DAPI (blue) to detect DNA. Low and high magnifications are presented. Scale bars: 25 μm. (C) RTqPCR analysis of *Itpkc* mRNA expression in various mouse tissues. (D) Immunodetection on protein extracts from four tissues isolated from an adult control mouse. Ald and gamma Tubulin (as loading control) antibodies were used to probe the membrane.

expression was rather ubiquitous, with a high expression in testis, large intestine, kidney, brain and spleen. Expression was intermediate in stomach, salivary gland, liver, thymus, lung, caecum and small intestine. Trachea and epididymis expressed only very low amount of *Itpkc* mRNA. ITPKC protein expression was next investigated by immunodetection in mouse liver, intestine, lung and testis with the Ald antibody (Fig. 1d). A strong signal at ~90 kDa was detected in intestine and testis, and a weak signal was present in liver and lung. Cellular *Itpkc* mRNA and protein expression were analyzed in mouse intestine, testis, lung, brain and kidney by *in situ* hybridization (ISH) using a mouse *Itpkc* RNA probe, and/or by immunofluorescence (IF) using the GS2 antibody. In intestine cryosections, *Itpkc* mRNA was detected in the epithelium which limits the intestine lumen (Fig. 2a). Indeed, punctuate dots, which are specific ISH signals in this assay, were nearly exclusively limited to the surface epithelium in both large and small intestines. Using the GS2 antibody on large intestine cryosections, we observed that the IF signal was also limited to the simple columnar epithelium, with a higher intensity signal present between the nucleus and the apical pole of the epithelium (Fig. 2b). The GS2 IF signal in the epithelium co-localized with Ezrin, a protein which is essential for epithelial organization and villus morphogenesis in the intestine (Fig. 2b). Isolated large intestine epithelial cells showed a polarized GS2 IF staining (Fig. 2c). In testis cryosections, *Itpkc* mRNA was detected in the seminiferous tubules, particularly in the peripheral region of the tubules (Fig. 3a). The GS2 IF signal was also detected in the seminiferous tubules, as punctuate dots next to the nucleus (Fig. 3b). GS2 IF analysis of motile sperm isolated from mouse epididymis revealed a single punctuate dot signal at the junction between the head and the mid piece of the spermatozoon, next to the nucleus and centrin local-ization (Fig. 3c). In lung and trachea cryosections, punctuate dots were nearly exclusively limited to the bronchial and tracheal epithelia, respectively (Fig. 4a and b). A non-dotted, linear ISH background signal of unknown origin was also detected in the tissue sustaining these two epithelia. We observed that the GS2 IF signal was also limited to the bronchial and tracheal epithelia, labeling most epithelial cells (Fig. 4c). The GS2 IF signal was clearly present in acetylated tubulin+ multiciliated cells of the bronchial epithelium (Fig. 4c). The GS2 IF signal was also analyzed in mouse tracheal epithelial cell (MTEC) culture. In this culture, once tracheal epithelial cells have reached confluence onto a Transwell filter, an air-liquid interface is created, allowing beating multicilia to develop within 5−11 days in ~50% of the cells. In this model, we observed that the GS2 IF signal was exclusively present in acetylated Tubulin+ multiciliated epithelial cells (Fig. 4d). Acetylated Tubulin− non-ciliated epithelial cells were negative for GS2 IF. Finally, we also investigated GS2 IF on mouse kidney and brain cryosections (Fig. 5a and b, respectively). In these two organs, GS2 IF signals localized within Ezrin+ renal proximal tubule epithelial cells and within Ezrin+ ependymal cells lining cerebral ventricles (Fig. 5). In these two cell types, Ezrin is a marker of the microvilli containing brush border and of multicilia, respectively.

Together, our study indicates that the ITPKC protein is not uniformly expressed in mouse tissues, but is rather expressed in specific cell types within tissues, like in epithelia. Interestingly, all cells which are positive for Itpkc in the present study are either multiciliated (tracheal and bronchial epithelia, brain ependymal cells), or have developed microvilli within a brush
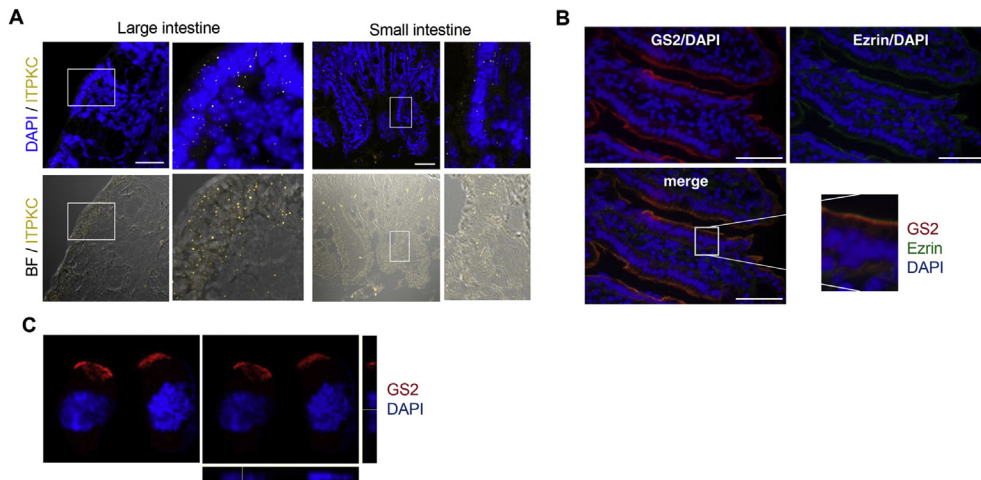
Fig. 2. Analysis of *Itpkc* mRNA and protein expression in small and large intestines isolated from an adult control mouse: (A) Large and small intestine cryosections were analyzed by ISH with a mouse *Itpkc* oligo RNAscope probe. Yellow punctuate dots are specific ISH signals in this assay. Cryosections were counterstained with DAPI (which stains DNA). Bright fields (BF) are also presented. Low and high magnifications are shown. Scale bars: 50 μm. (B) Large intestine cryosections were incubated with GS2 (red) or Ezrin (green) antibodies and counterstained with DAPI (blue) to detect DNA. Low and high magnifications are presented. Scale bars: 50 μm. (C) Isolated large intestine cells detached from the epithelium were incubated with the GS2 antibody (red) and counterstained with DAPI.
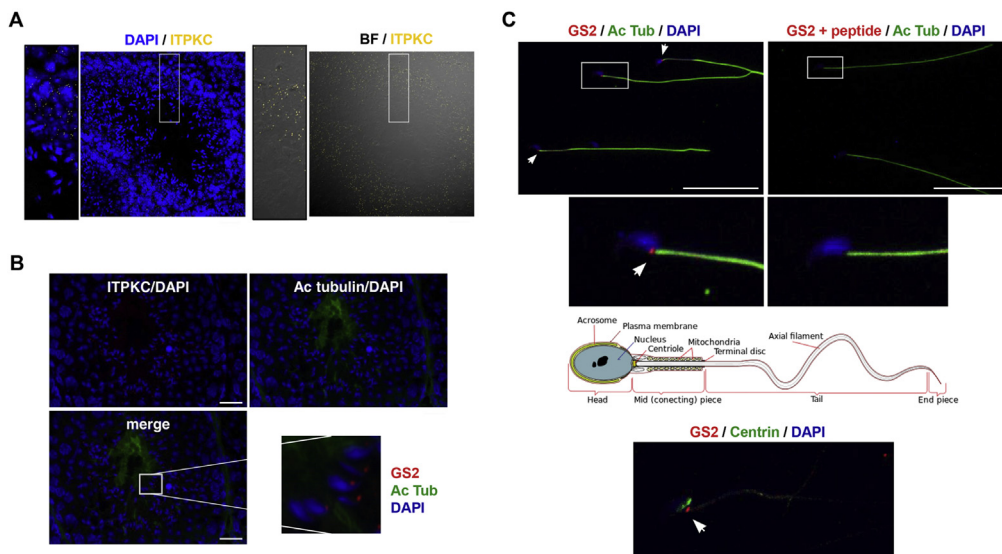
Fig. 3. Analysis of Itpkc mRNA and protein expression in testis and sperm isolated from and adult control mouse: (A) Testis cryosections were analyzed by ISH with a mouse *Itpkc* oligo RNAscope probe. Yellow punctuate dots are specific ISH signals in this assay. Cryosections were counterstained with DAPI (which stains DNA). Bright fields (BF) are also presented. Low and high magnifications are shown. Scale bars: 50 μm. (B) Testis cryosections were incubated with GS2 (ITPKC, red) and acetylated Tubulin (green) antibodies and counterstained with DAPI. Low and high magnifications are presented. Scale bars: 50 μm. (C) Upper images: spermatozoa were isolated from adult mouse epididymis and stained with GS2 preincubated or not with the immunizing peptide (red, white arrows) and acetylated Tubulin (green) antibodies, and counterstained with DAPI (blue) to detect DNA. Low and high magnifications are presented. Scale bars: 50 μm. Intermediate image: a spermatozoon picture is presented with head, mid connecting piece and tail. Lower image: a spermatozoon is stained with GS2 (red, white arrow), Centrin (green) and DAPI (blue, DNA).

border (small and large intestine, and kidney proximal tubule cells) or a flagellum (spermatozoa), suggesting a role for the ITPKC protein in the development or the function of these specialized cellular structures.

3.3. Functional analysis of ITPKC in multiciliated tracheal epithelial cells and sperm cells

ITPKC protein function was investigated in *Itpkc*^{+/+} and *Itpkc*^{−/−} mice (Pouillon et al., 2003). We previously reported that, in these *Itpkc*^{−/−} mice, a neomycin resistance cassette was replacing a 1.1 kb genomic fragment comprising the 3′ part of the first coding exon and the 5′ part of the first intron (Pouillon et al., 2003). RT-PCR analysis on testis mRNA with primers located in
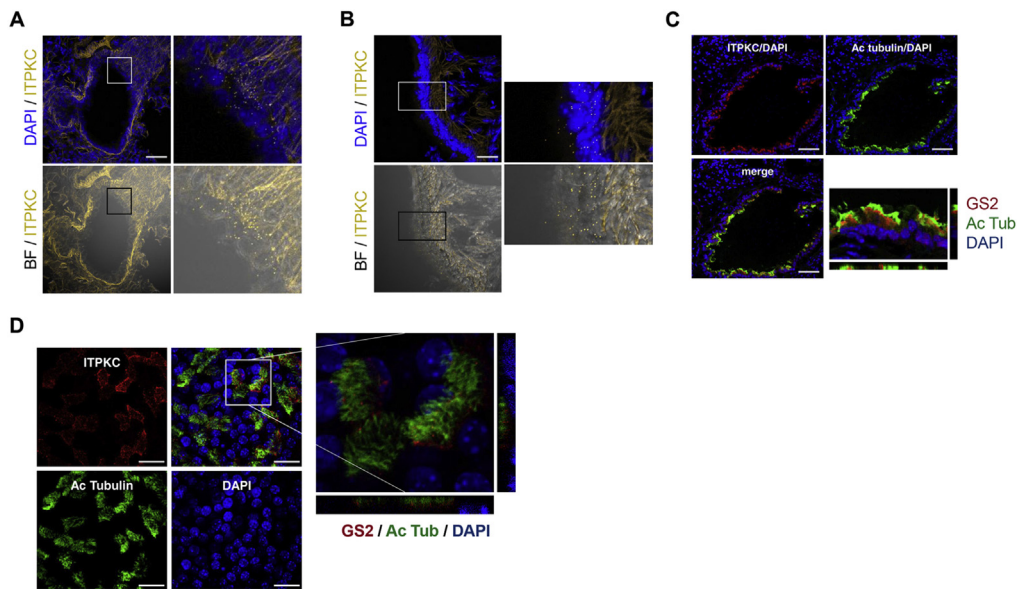
Fig. 4. Analysis of *Itpkc* mRNA and protein expression in lung, trachea and MTEC isolated from an adult control mouse: Lung (A) and trachea (B) cryosections were analyzed by ISH with a mouse *Itpkc* oligo RNAscope probe. Yellow punctuate dots are specific ISH signals in this assay. Cryosections were counterstained with DAPI (which stains DNA). Bright fields (BF) are also presented. Low and high magnifications are shown. Scale bars: 50 μm. Lung cryosections (C) and MTEC (D) were incubated with GS2 (red) and acetylated Tubulin (green) antibodies and counterstained with DAPI (blue) to detect DNA. Low and high magnifications are presented. Scale bars: 50 μm (C) or 20 μm (D).
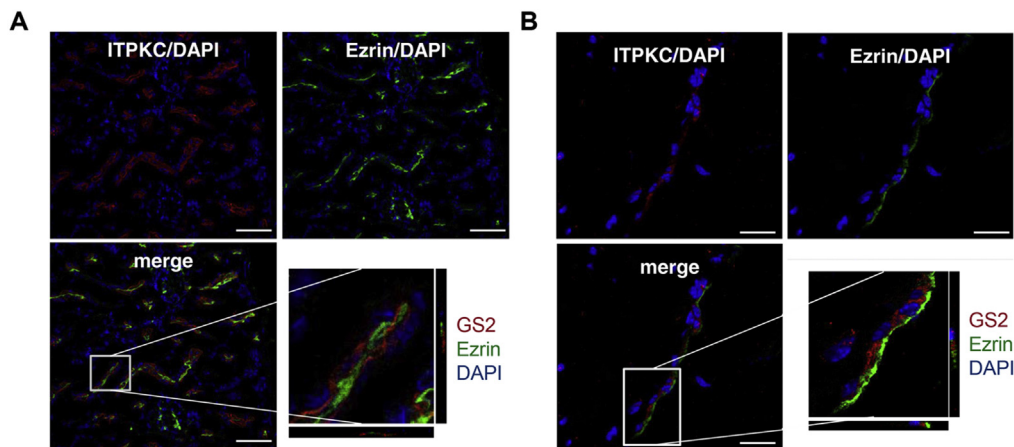
Fig. 5. Analysis of ITPKC protein expression in kidney and brain ependymal cells isolated from an adult control mouse: Kidney (A) and brain (B) cryosections were incubated with GS2 (red) or Ezrin (green) antibodies and counterstained with DAPI (blue) to detect DNA. For brain cryosections, only ependymal cells lining cerebral ventricles are presented. Low and high magnifications are presented. Scale bars: 50 μm.

the first and the third exons did not yield an amplicon in the mutant mice, on the contrary to *Itpkc*$^{+/+}$ and *Itpkc*$^{+/-}$ mice (Pouillon et al., 2003). Importantly, Ins(1,4,5)P3 3-kinase activity was detected but significantly decreased in intestine protein extracts from *Itpkc*$^{-/-}$ mice, as compared with *Itpkc*$^{+/+}$ and *Itpkc*$^{+/-}$ mice (Pouillon et al., 2003). As expected from these previous results, immunodetection analysis of brain and lung protein extracts with the Ald antibody revealed a ~90 kD signal in *Itpkc*$^{+/+}$ mice, but not in *Itpkc*$^{-/-}$ mice (Fig. 6a). A similar result was obtained when analyzing MTEC protein extracts from *Itpkc*$^{+/+}$ and *Itpkc*$^{-/-}$ mice with the GS2 antibody (Fig. 6b). No obvious phenotype has been previously detected in *Itpkc*$^{-/-}$ mice: length, weight, survival as well as macroscopic and microscopic organs examination and T lymphocyte development were normal in these mutant mice (Pouillon et al., 2003). Since our expression studies suggest a link between ITPKC and specialized cellular structures like multicilium and flagellum, morphology and function of these structures was investigated in the tracheal epithelium and spermatozoids. Scanning electron microscopy (SEM) analysis of multicilia present on tracheal
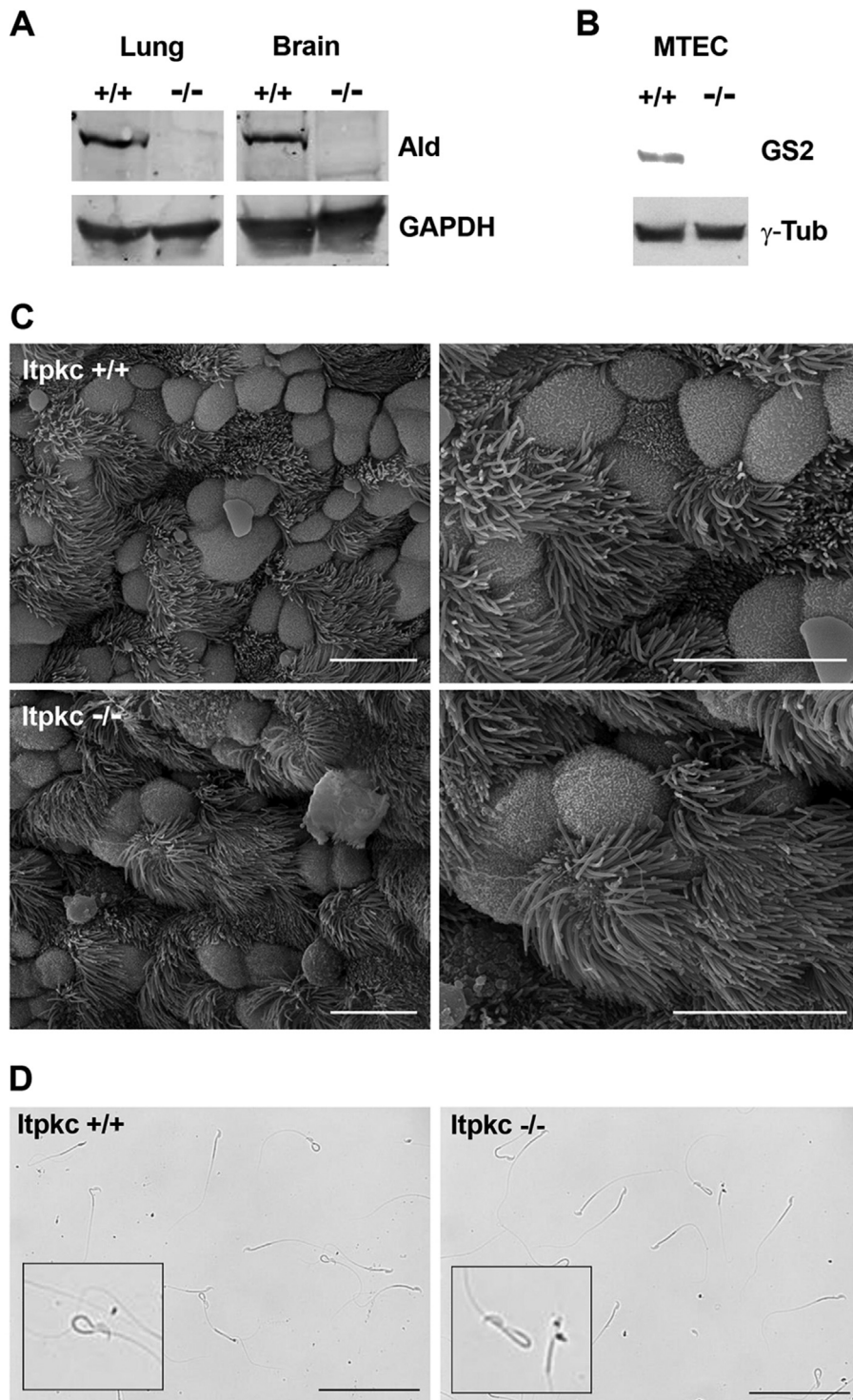
Fig. 6. Analysis of _Itpkc_+/+ and _Itpkc_−/− mice: Immunodetection on protein extracts isolated from _Itpkc_+/+ (+/+) and _Itpkc_−/− (−/−) lung (A), brain (A) and MTEC (B). Ald and GAPDH (A) or GS2 and gamma Tubulin (B) antibodies were added to the membrane. A specific ITPKC signal was detected at ~90 kDa. (C) SEM analysis of multicilia present on tracheal epithelial cells from _Itpkc_+/+ and _Itpkc_−/− mice. Low (scale bars: 20 μm) and high (scale bars: 10 μm) magnifications are presented. (D) _Itpkc_+/+ (left panel) and _Itpkc_−/− (right panel) spermatozoa were isolated from adult mouse epididymis. Scale bars = 100 μm. Insets show higher magnification on a few spermatozoa.

epithelial cells from _Itpkc_+/+ and _Itpkc_−/− mice revealed no obvious difference (Fig. 6c): a similar percentage of tracheal

epithelial cells presented with a multicilium ($Itpkc^{+/+}$: 48 ± 5% of multiciliated cells, $Itpkc^{-/-}$: 51 ± 7% of multiciliated cells; mean ± SEM, P = 0.52), and multicilia were similar in term of cilia number, length and diameter (Fig. 6c). The tracheal multiciliary beating frequency was analyzed in the MTEC model. Again, no significant difference was detected for multiciliary beating frequency between $Itpkc^{+/+}$ (9.3 ± 2.2 Hz, mean ± SEM) and $Itpkc^{-/-}$ (10.0 ± 3.5 Hz, mean ± SEM; P = 0.44) MTEC. Epididymal spermatozoa were isolated from 8-week old $Itpkc^{+/+}$ and $Itpkc^{-/-}$ male mice. No obvious morphological defect was detected in $Itpkc^{-/-}$ spermatozoa, as compared to $Itpkc^{+/+}$ spermatozoa (Fig. 6d). In non-stimulated conditions, the percentage of spermatozoa with a 'fishhook' like shape flagellum was similar in $Itpkc^{+/+}$ (16 ± 3%, mean ± SEM) and $Itpkc^{-/-}$ (15 ± 3%, mean ± SEM; P = 0.55) mice. Accordingly, reproductive capacity of male $Itpkc^{-/-}$ mice was normal: $Itpkc^{-/-}$ mice intercrosses gave litters of normal size, compared with $Itpkc^{+/+}$ intercrosses ($Itpkc^{+/+}$: 5.8 ± 1.8 newborns per litter, $Itpkc^{-/-}$: 5.3 ± 1.9 newborns per letter; mean ± SEM, 20 litters, P = 0.67).

4. Conclusions

Here, for the first time, we define the expression of Itpkc mRNA and protein in various mouse tissues using ISH and IF analysis on tissue sections. We found that ITPKC is not uniformly expressed in mouse tissues, but it is rather expressed in specific cell types within the studied tissues. Interestingly, cells positive for ITPKC in these tissues express either a multicilium, microvilli forming a brush border or a flagellum. This is specific for ITPKC and was not observed with ITPKA and ITPKB. The mouse endogenous ITPKC protein was never detected in the nucleus, in contrast to previously reported data of transfected rat and human ITPKC in NRK 52E renal cells (Nalaskowski et al., 2003, 2006). We also analyzed multiciliated tracheal epithelial cells and spermatozoa for ITPKC protein function in our $Itpkc^{+/+}$ and $Itpkc^{-/-}$ mice. Unfortunately, no significant difference was observed between control and mutant mice for any of the parameters tested, leaving the exact *in vivo* function of the last reported isoenzyme of is third Ins(1,4,5)P3 3-kinase still open.

Acknowledgments

Appendix A. Supplementary data

Supplementary data related to this article can be found at http://dx.doi.org/10.1016/j.jbior.2016.03.001.

References

Burgner, D., Davila, S., Breunis, W.B., Ng, S.B., Li, Y., Bonnard, C., Ling, L., Wright, V.J., Thalamuthu, A., Odam, M., Shimizu, C., Burns, J.C., Levin, M., Kuijpers, T. W., Hibberd, M.L., International Kawasaki Disease Genetics Consortium, 2009. A genome-wide association study identifies novel and functionally related susceptibility Loci for Kawasaki disease. PLoS Genet. 5, e1000319.

Burnett, L.A., Anderson, D.M., Rawls, A., Bieber, A.L., Chandler, D.E., 2011. Mouse sperm exhibit chemotaxis to allurin, a truncated member of the cysteine-rich secretory protein family. Dev. Biol. 360, 318–328.

Choi, K.Y., Kim, H.K., Lee, S.Y., Moon, K.H., Sim, S.S., Kim, J.W., Chung, H.K., Rhee, S.G., 1990. Molecular cloning and expression of a complementary DNA for inositol 1,4,5-trisphosphate 3-kinase. Science 248, 64–66.

Communi, D., Vanweyenberg, V., Erneux, C., 1997. D-myo-inositol 1,4,5-trisphosphate 3-kinase A is activated by receptor activation through a calcium: calmodulin-dependent protein kinase II phosphorylation mechanism. EMBO J. 16, 1943–1952.

Dewaste, V., Pouillon, V., Moreau, C., Shears, S., Takazawa, K., Erneux, C., 2000. Cloning and expression of a cDNA encoding human inositol 1,4,5-trisphosphate 3-kinase C. Biochem. J. 352, 343–351.

Erneux, C., Ghosh, S., Koenig, S., 2016. Inositol(1,4,5)P3 3-kinase isoenzymes: catalytic properties and importance of targeting to F-actin to understand function. Adv. Biol. Regul. 60, 135–143.

Fukuda, N., Yomogida, K., Okabe, M., Touhara, K., 2004. Functional characterization of a mouse testicular olfactory receptor and its role in chemosensing and in regulation of sperm motility. J. Cell. Sci. 117, 5835–5845.

Hata, A., Onouchi, Y., 2009. Susceptibility genes for Kawasaki disease: toward implementation of personalized medicine. J. Hum. Genet. 54, 67–73.

Khor, C.C., Davila, S., Breunis, W.B., Lee, Y.C., Shimizu, C., Wright, V.J., Yeung, R.S., Tan, D.E., Sim, K.S., Wang, J.J., Wong, T.Y., Pang, J., Mitchell, P., Cimaz, R., Dahdah, N., Cheung, Y.F., Huang, G.Y., Yang, W., Park, I.S., Lee, J.K., Wu, J.Y., Levin, M., Burns, J.C., Burgner, D., Kuijpers, T.W., Hibberd, M.L., Hong Kong−Shanghai Kawasaki Disease Genetics Consortium, Korean Kawasaki Disease Genetics Consortium, Taiwan Kawasaki Disease Genetics Consortium, International Kawasaki Disease Genetics Consortium, US Kawasaki Disease Genetics Consortium, Blue Mountains Eye Study, 2011. Genome-wide association study identifies FCGR2A as a susceptibility locus for Kawasaki disease. Nat. Genet. 43, 1241–1246.

Kuo, H.C., Yang, K.D., Juo, S.H., Liang, C.D., Chen, W.C., Wang, Y.S., Lee, C.H., His, E., Yu, H.R., Woon, P.Y., Lin, I.C., Huang, C.F., Hwang, D.Y., Lee, C.P., Lin, L.Y., Chang, W.P., Chang, W.C., 2011. ITPKC single nucleotide polymorphism associated with the Kawasaki disease in a Taiwanese population. PLoS One 6, e17370.

Lin, M.T., Wang, J.K., Yeh, J.I., Sun, L.C., Chen, P.L., Wu, J.F., Chang, C.C., Lee, W.L., Shen, C.T., Wang, N.K., Wu, C.S., Yeh, S.Z., Chen, C.A., Chiu, S.N., Wu, M.H., 2011. Clinical implication of the C allele of the Itpkc gene SNP rs28493229 in Kawasaki disease. Pediatr. Infect. Dis. J. 30, 148–152.

Nalaskowski, M.M., Bertsch, U., Fanick, W., Stockebrand, M.C., Schmale, H., Mayr, G.W., 2003. Rat inositol 1,4,5-trisphosphate 3-kinase C is enzymatically specialized for basal cellular inositol trisphosphate phosphorylation and shuttles actively between nucleus and cytoplasm. J. Biol. Chem. 278, 19765–19776.

Nalaskowski, M.M., Windhorst, S., Stockebrand, M.C., Mayr, G.W., 2006. Subcellular localisation of human inositol 1,4,5-trisphosphate 3-kinase C: species-specific use of alternative export sites for nucleo-cytoplasmic shuttling indicates divergent roles of the catalytic and N-terminal domains. Biol. Chem. 387, 583—593.

Onouchi, Y., Gunji, T., Burns, J.C., Shimizu, C., Newburger, J.W., Yashiro, M., Nakamura, Y., Yanagawa, H., Wakui, K., Fukushima, Y., Kishi, F., Hamamoto, K., Terai, M., Sato, Y., Ouchi, K., Saji, T., Nariai, A., Kaburagi, Y., Yoshikawa, T., Suzuki, K., Tanaka, T., Nagai, T., Cho, H., Fujino, A., Sekine, A., Nakamichi, R., Tsunoda, T., Kawasaki, T., Nakamura, Y., Hata, A., 2008. ITPKC functional polymorphism associated with Kawasaki disease susceptibility and formation of coronary artery aneurysms. Nat. Genet. 40, 35—42.

Onouchi, Y., Suzuki, Y., Suzuki, H., Terai, M., Yasukawa, K., Hamada, H., Suenaga, T., Honda, T., Honda, A., Kobayashi, H., Takeuchi, T., Yoshikawa, N., Sato, J., Shibuta, S., Miyawaki, M., Oishi, K., Yamaga, H., Aoyagi, N., Iwahashi, S., Miyashita, R., Murata, Y., Ebata, R., Higashi, K., Ozaki, K., Sasago, K., Tanaka, T., Hata, A., 2013. ITPKC and CASP3 polymorphisms and risks for IVIG unresponsiveness and coronary artery lesion formation in Kawasaki disease. Pharmacogenomics J. 13, 52—59.

Peng, Q., Chen, C., Zhang, Y., He, H., Wu, Q., Liao, J., Li, B., Luo, C., Hu, X., Zheng, Z., Yang, Y., 2012. Single-nucleotide polymorphism rs2290692 in the 3′UTR of ITPKC associated with susceptibility to Kawasaki disease in a Han Chinese population. Pediatr. Cardiol. 33, 1046—1053.

Pouillon, V., Hascakova-Bartova, R., Pajak, B., Adam, E., Bex, F., Dewaste, V., Van Lint, C., Leo, O., Erneux, C., Schurmans, S., 2003. Inositol 1,3,4,5-tetrakisphosphate is essential for T lymphocyte development. Nat. Immunol. 4, 1136—1143.

Pouillon, V., Maréchal, Y., Frippiat, C., Erneux, C., Schurmans, S., 2013. Inositol 1,4,5-trisphosphate 3-kinase B (Itpkb) controls survival, proliferation and cytokine production in mouse peripheral T cells. Adv. Biol. Regul. 53, 39—50.

Saiardi, A., Caffrey, J.J., Snyder, S.H., Shears, S.B., 2000. Inositol polyphosphate multikinase (ArgRIII) determines nuclear mRNA export in Saccharomyces cerevisiae. FEBS Lett. 468, 28—32.

Schurmans, S., Pouillon, V., Maréchal, Y., 2011. Regulation of B cell survival, development and function by inositol 1,4,5-trisphosphate 3-kinase B (Itpkb). Adv. Enzyme Regul. 51, 66—73.

Schurmans, S., Polizzi, S., Scoumanne, A., Sayyed, S., Molina-Ortiz, P., 2015. The Ras/Rap GTPase activating protein RASA3: from gene structure to in vivo functions. Adv. Biol. Regul. 5, 153—161.

Takazawa, K., Lemos, M., Delvaux, A., Lejeune, C., Dumont, J.E., Erneux, C., 1990. Rat brain inositol 1,4,5-trisphosphate 3-kinase. Ca2+-sensitivity, purification and antibody production. Biochem. J. 268, 213—217.

Takazawa, K., Perret, J., Dumont, J.E., Erneux, C., 1991. Molecular cloning and expression of a new putative inositol 1,4,5-trisphosphate 3-kinase isoenzyme. Biochem. J. 278, 883—886.

Vanweyenberg, V., Communi, D., D'Santos, C.S., Erneux, C., 1995. Tissue- and cell-specific expression of Ins(1,4,5)P3 3-kinase isoenzymes. Biochem. 306, 429—435.

York, J.D., 2006. Regulation of nuclear processes by inositol polyphosphates. Biochim. Biophys. Acta 1761, 552—559.

You, Y., Richer, E.J., Huang, T., Brody, S.L., 2002. Growth and differentiation of mouse tracheal epithelial cells: selection of a proliferative population. Am. J. Physiol. Lung Cell. Mol. Physiol. 283, L1315—L1321.